Title	Transcriptional regulatory factor X6 (Rfx6) increases gastric inhibitory polypeptide (GIP) expression in enteroendocrine K-cells and is involved in GIP hypersecretion in high fat diet-induced obesity.
Author(s)	Suzuki, Kazuyo; Harada, Norio; Yamane, Shunsuke; Nakamura, Yasuhiko; Sasaki, Kazuki; Nasteska, Daniela; Joo, Erina; Shibue, Kimitaka; Harada, Takanari; Hamasaki, Akihiro; Toyoda, Kentaro; Nagashima, Kazuaki; Inagaki, Nobuya
Citation	The Journal of biological chemistry (2013), 288(3): 1929-1938
Issue Date	2013-01-18
URL	http://hdl.handle.net/2433/182055
Right	© 2013 by The American Society for Biochemistry and Molecular Biology, Inc.
Type	Journal Article
Textversion	author

Transcriptional factor regulatory factor X 6 (Rfx6) increases gastric inhibitory polypeptide (GIP) expression in enteroendocrine K-cells and is involved in GIP hypersecretion in high-fat diet-induced obesity

Kazuyo Suzuki, Norio Harada, Shunsuke Yamane, Yasuhiko Nakamura, Kazuki Sasaki, Daniela Nasteska, Erina Joo, Kimitaka Shibue, Takanari Harada, Akihiro Hamasaki, Kentaro Toyoda, Kazuaki Nagashima, and Nobuya Inagaki

Department of Diabetes and Clinical Nutrition,
Graduate School of Medicine, Kyoto University, Kyoto, Japan

*Running title: *Rfx6 increases GIP mRNA expression in K-cells*

Corresponding Author. Address: Nobuya Inagaki, Department of Diabetes and Clinical Nutrition, Graduate School of Medicine, Kyoto University, 54 Kawahara-cho, Shogoin, Sakyo-ku, Kyoto 606-8507, Japan. Tel: +81(Japan)-75-751-3562, Fax: +81(Japan)-75-751-6601
E-mail: inagaki@metab.kuhp.kyoto-u.ac.jp

Key words: GIP; K-cell; Rfx6; Pdx1; obesity

Background: Gastric inhibitory polypeptide (GIP) secreted from enteroendocrine K-cells potentiates insulin secretion and induces energy accumulation into adipose tissue.
Results: Transcriptional factor Rfx6 is expressed in K-cells and increases GIP expression. Rfx6 expression is upregulated in K-cells of obese mice.
Conclusion: Rfx6 plays critical roles in GIP expression and hypersecretion in obesity.
Significance: Gene analysis of K-cells isolated from GIP-GFP knock-in mice enabled identification of Rfx6.

SUMMARY
Gastric inhibitory polypeptide (GIP) is an incretin released from enteroendocrine K-cells in response to nutrient ingestion. GIP potentiates glucose-stimulated insulin secretion and induces energy accumulation into adipose tissue, resulting in obesity. Plasma GIP levels are reported to be increased in the obese state. However, the molecular mechanisms of GIP secretion and high-fat diet (HFD)-induced GIP hypersecretion remain unclear, primarily due to difficulties in separating K-cells from other intestinal epithelial cells *in vivo*. In the present study, GIP-GFP knock-in mice that enable us to visualize K-cells by EGFP were established. Microarray analysis of isolated K-cells from these mice revealed that transcriptional factor regulatory factor X 6 (Rfx6) is expressed exclusively in K-cells. *In vitro* experiments using mouse intestinal cell line STC-1 showed that knockdown of Rfx6 decreased mRNA expression, cellular content, and secretion of GIP. Rfx6 bound to the region in GIP promoter that regulates GIP promoter activity and over-expression of Rfx6 increased GIP mRNA expression. HFD induced obesity and GIP hypersecretion in GIP-GFP heterozygous mice *in vivo*. Immunohistochemical and flow cytometry analysis showed no significant difference in K-cell number between control-fat diet (CFD)-fed and HFD-fed mice. However, GIP content in upper small intestine and GIP mRNA expression in K-cells were significantly increased in HFD-fed mice compared to those in CFD-fed mice. Furthermore, expression levels of Rfx6 mRNA were increased in K-cells of HFD-fed mice. These results suggest that Rfx6 increases GIP expression and content in K-cells and is involved in GIP hypersecretion in HFD-induced obesity.

Obesity leads to insulin resistance characterized by fasting hyperinsulinemia and excessive insulin secretion to maintain euglycemia after meal ingestion (1). Obesity is an important risk factor in progression to type 2 diabetes mellitus (2) as well as

cardiovascular disease (3), and reduction of obesity can normalize hyperinsulinemia and impede the progression of diabetes and arteriosclerosis.

Gastric inhibitory polypeptide, also called glucose-dependent insulinotropic polypeptide (GIP), and glucagon-like peptide-1 (GLP-1) are the incretins, peptide hormones released from the gastrointestinal tract into circulation in response to meal ingestion that potentiate glucose-stimulated insulin secretion (4, 5). GIP is secreted from enteroendocrine K-cells located in the duodenum and upper small intestine; GLP-1 is secreted from enteroendocrine L-cells located in lower small intestine and colon. GIP binds to the GIP receptor (GIPR) on the surface of pancreatic β-cells, adipose tissue and osteoblasts, and stimulates insulin secretion (6), fat accumulation (7), and bone formation (8), respectively, by increasing the level of intracellular adenosine 3',5'-monophosphate (cAMP).

It was reported previously that GIPR-deficient mice exhibit insufficient compensatory insulin secretion upon high-fat loading (9), suggesting that GIP plays a critical role in maintaining blood glucose levels by hypersecretion of insulin in diet-induced obesity. We also reported that sensitivity of GIPR to GIP in β-cells is increased in high-fat diet (HFD)-induced obese mice (10). In addition, GIPR is expressed in adipose tissue (11), and increases glucose and triglyceride uptake in fat cells (12, 13). Thus, GIP has both direct and indirect effects on the accumulation of energy into adipose tissue. Some studies report that GIP secretion is increased in obesity (7, 14, 15, 16) and that pancreatic and duodenal homeobox 1 (Pdx1) , which is known to be an important transcription factor in pancreatic development and pancreatice β-cell maturation (17), has a critical role in GIP production in K-cells (18, 19). However, the mechanisms involved in GIP hypersecretion from K-cells in obesity remain unclear due to difficulties in separating these cells from other intestinal epithelial cells *in vivo*.

In the present study, we investigated expression of various genes in K-cells by using GIP-GFP knock-in (GIP-GFP) mice in which K-cells can be visualized by EGFP fluorescence. We found that the transcriptional factor regulatory factor X 6 (Rfx6) is expressed exclusively in K-cells of upper small intestine and is involved in GIP mRNA expression in the mouse small intestinal cell line STC-1. Furthermore, expression of Rfx6 as well as Pdx1 was found to be increased in K-cells of HFD-induced obese mice. Thus, GIP expression is stimulated by both Rfx6 and Pdx1, suggesting that these transcriptional factors play an important role in both GIP expression and GIP hypersecretion in HFD-induced obesity.

EXPERIMENTAL PROCEDURES

Animals— We designed targeting vector constructs as short -EGFP-polyA-loxp-Neo-loxp-long cassettes using mouse B6N BAC Clone (ID: RP23-31E4 and RP23-383D10). A diphtheria toxin A expression cassette for negative selection was attached to the 3’ end of the GIP sequence in the targeting vector. Next, the targeting vector was injected in embryonic stem cells from C57BL6 mice and a Neo resistance strain was established. The ES cells positive for the knock-in gene were selected by southern blot analysis. The established ES cells were then injected into the blastocyst in order to obtain chimeric mice. Finally, we generated hetero-mutant mice by mating the chimeric mice with wild C57BL6. The mice were housed in an air-controlled (temperature 25°C) room with dark–light cycle of 10 h and 14 h, respectively. Animal care and procedures were approved by the Animal Care Committee of Kyoto University.

GIP-GFP heterozygous mice (7 weeks of age) were fed control fat chow (CFD; 10% fat, 20% protein, and 70% carbohydrate by energy) or high fat chow (HFD; 60% fat, 20% protein, and 20% carbohydrate by energy) (Research Diets Inc., New Brunswick, NJ) for 8 weeks. Food intake, water intake, and body weight were measured.

Immunohistochemistry— Mouse upper small intestine samples were fixed in Bouin’s solution and transferred into 70% ethanol before processing through paraffin. Rehydrated paraffin sections were incubated overnight at 4°C with primary mouse

anti-GFP antibody (sc-9996, 1:100, Santa Cruz Biotechnology Inc., biotechnology, inc., CA) and rabbit anti-GIP antibody (T-4053, 1:100, Peninsula Laboratories, Inc., San Carlos, CA). Intestine samples and STC-1 cells (kindly provided by Prof. Hanahan, University of California, San Francisco) were embedded by Tissue-Tek O.C.T. compound 4583 (Sakura Fine Technical Co. Ltd. Tokyo, Japan) and immediately frozen in liquid nitrogen. Frozen sections (10 μm) on slides were air-dried and fixed in acetone for 5 min. Slides were then washed in PBS and blocked for 15 min in 3% BSA. They were incubated overnight at 4°C with primary antibody (Mouse anti-GIP antibody (1:100, kindly provided by Merck Millipore, Darmstadt, Germany) and goat anti-Rfx6 antibody (ABD28, 1:100, Merck Millipore)). The sections were incubated for 1 h at room temperature with secondary antibody. Images were taken using a fluorescent microscopy with a BZ-8100 system (KEYENCE Corporation, Osaka, Japan) and confocal microscopy with a LSM510META system (Carl Zeiss Co., Ltd., Jena, Germany).

Fifty representative mucous membranes from each slide were randomly selected and their mean length and GFP-positive cells were quantified using fluorescent microscopy images. In order to count GFP-positive cells, we distinguished the mucous membrane as villus, upper crypt or lower crypt.

Isolation of K-cells from mouse intestinal epithelium— Mouse upper small intestine was removed and washed by phosphate buffer saline (PBS). The intestine was cut into several round pieces and tied at one side with a thread. The pouch-like intestine was injected with Hanks balanced salt solution (HBSS) containing 0.5 mg / ml collagenase, clamped and incubated with CO_2 at 37°C for 10 min in Krebs-Ringer bicarbonate buffer (KRBB; 120 mM NaCl, 4.7 mM KCl, 1.2 mM $MgSO_4$, 1.2 mM KH_2PO_4, 2.4 mM $CaCl_2$, 20 mM $NaHCO_3$). The digested intestinal epithelium was collected into the tube filled with Roswell Park Memorial Institute (RPMI) medium and rinsed twice. The intestinal epithelium was cultured in a humidified incubator (95% air and 5% CO_2) at 37°C for 1 h. Afterwards, it was centrifuged at 180 x g for 5 min, resuspended in PBS twice and filtered with a cell strainer (352340, BD Falcon cell strainer, Becton Dickinson and Company, San Jose, CA). GFP-positive cells in the intestinal epithelium were analyzed using BD FACS Aria™ flow cytometer (Becton Dickinson and Company). Sorted cells were collected into vials containing medium at a rate of 2000 cells / tube.

Total RNA was extracted with PicoPure RNA isolation kit (Applied Biosystems, Inc, Alameda, CA) from sorted cells of GIP-GFP mice intestinal epithelium and treated with DNase (Qiagen Inc., Valencia, CA). Microarray analysis was performed using GeneChip Mouse Genome 430 2.0 Array (Affymetrix Inc., Fremont, CA).

Glucose tolerance test (OGTT) and GIP assay— After a 16-h fasting period, oral glucose tolerance tests (OGTTs) (1 g / kg body weight) were performed. Blood samples were taken at the indicated times (0, 15, 30, 60 and 120 min after glucose loading) and blood glucose levels, plasma insulin levels, and plasma total GIP concentrations were measured. Blood glucose levels were determined by the glucose oxidase method (Sanwa Kagaku Kenkyusho CO. LTD., Nagoya, Japan). Plasma insulin levels were determined using enzyme immunoassay (Shibayagi, Gumma, Japan). Plasma total GIP levels were determined using ELISA assay kit (Merck Millipore).

For measurement of GIP content in mouse upper small intestine, the mice were killed at 15 weeks of age after 8 weeks of CFD or HFD feeding. The intestine was rapidly removed and washed by PBS. After measurement of the weight, samples were extracted with 5ml / g acid ethanol, and GIP levels were measured (15).

Quantitative RT-PCR— Complementary DNA (cDNA) was prepared by reverse transcriptase (Invitrogen, Carlsbad, CA) with an oligo (dT) primer (Invitrogen). Messenger RNA (mRNA) levels were measured by quantitative RT-PCR using ABI PRISM 7000 Sequence Detection System (Applied Biosystems Inc.). PCR analyses were carried out using the oligonucleotide primers. SYBR Green PCR Master Mix (Applied Biosystems Inc.) was prepared for PCR run. Thermal cycling conditions were denaturation at 95°C for 10 min followed by 50 cycles at 95°C for 15 sec and 60°C for 1 min. C-terminal

and N-terminal primers of target molecules were designed as follows: GIP; Forward, 5'- gtggctttgaagacctgctc -3', reverse, 5'- ttgttgtcggatcttgtcca -3', GFP; 5'- gtggctttgaagacctgctc -3', reverse, 5'- tttacgtcgccgtccagctcg -3', GLP-1; 5'- tgaagacaaacgccactcac -3', reverse, 5'- tcatgacgtttggcaatgtt -3', Pdx1; 5'- gacctttcccgaatggaa -3, 5'- cttgttttcctcgggttc -3', Rfx1; 5'- gcagccagaagcagtatgtg -3', reverse, 5'- tggcttctgacacagtctcact -3', Rfx2; 5'- cagaactccgagggaggag -3', reverse, 5'- ggagggtgagtgtctgcatc -3', Rfx3; 5'- cgtcacaggaggacaactca -3', reverse, 5'- cagacttttgcagcgtctca -3', Rfx4; 5'- ccgaatacactggccttagc -3', reverse, 5'- atgggtgctcctcatacagg -3', Rfx5; 5'- tctaccttcagctcccatcg -3', reverse, 5'- ggcaggtatccatgtgctct -3', Rfx6; 5'- acagacacggaatctgacat -3', reverse, 5'- ctctaccacagtgtccaacc -3', Rfx7; 5'- cgctctgcaacacaagatca -3', reverse, 5'- gaccagaaggcagttgaagg -3', GAPDH; 5'- aaatggtgaaggtcggtgtg -3', reverse, 5'- tcgttgatggcaacaatctc -3',

Cell culture and small interfering RNA (siRNA) transfection into STC-1 cells— STC-1 cells, mouse small intestinal cell line, were cultured in Dulbeco's modified Eagle's medium (DMEM) (Sigma-Aldrich Co. LLC, St Louis, MO) supplemented with 10% heat-inactivated fetal calf serum, 100 IU / ml penicillin and 100 μg / ml streptomycin at 37◦C in a humidified atmosphere (5% CO_2 and 95% air). siRNA transfection StealthTM siRNAs were synthesized (Invitrogen). The sequences of siRNAs specific for Rfx6 and Pdx1 are shown as follows: Pdx1; caguacuacgcggccacacagcucu and agagcuguguggccgcguaguacug, Rfx6; ggugaaugccaugguaucugauauu and aauaucagauaccauggcauucacc. Cultured STC-1 cells were trypsinized, suspended with DMEM medium without antibiotics, mixed with Opti-MEM (Invitrogen) containing siRNA and Lipofectamine TM2000 (Invitrogen), plated on 12-well dishes, and then incubated at 37°C in a CO_2 incubator. The amounts of STC-1 cells were 1 x 10^6 cells / well. Medium was replaced with 1 ml DMEM containing antibiotics about 5-6 h after transfection. RT-PCR was performed 48 h after transfection.

Plasmid construction and transfection into STC-1 cells— The cDNA fragment of mouse Rfx6 protein was obtained from mouse (C57BL / 6) islets by RT-PCR. The cDNA fragment of Rfx6 was cloned into pCMV vector (Clontech Laboratories, Mountain View, CA). Expression plasmids of Rfx6 cDNA was transfected into STC-1 cells using Lipofectamine TM2000 (Invitrogen). Plasmid (8 μg / well) was diluted into Opti-MEM, and Lipofectamine TM2000 was added and incubated at room temperature for 20 minutes. After incubation, the mixture was added to STC-1 cells (1 x 10^6 cells / well). RT-PCR was performed 48 h after transfection.

Measurement of incretin release and cellular content in STC-1 cells— For incretin release assays, DMEM media were collected from STC-1 cells cultured on 12-well dishes about 42-43 h after changing the medium (48 h after transfection). Media were centrifuged at 3,000 x g for 10 min and the supernatant was collected. Total GIP and Total GLP-1 levels were measured by ELISA methods (Millipore and Meso Scale Discovery (Gaithersburg, MD), respectively) as incretin release from STC-1 cells.

To determine incretin content, STC-1 cells cultured on 12-well dishes (48 h after transfection) were washed with PBS and were homogenized in 0.5 ml of 0.1 N HCl and extracted at RT for 10 min, after which the supernatant was collected and centrifuged at 3,000 x g for 10 min. Incretin and protein levels were measured by ELISA assay (GIP and GLP-1) and Bradford reagent (Bio-Rad Laboratories, Inc, Hercules, CA), respectively.

Yeast one-hybrid assay— Yeast one-hybrid assays were performed using the Matchmaker Gold Yeast One-Hybrid Library Screening System (Clontech Laboratories Inc., Mountain View, CA) according to the manufacturer's protocol. The GIP promoter fragments shown in Fig.4A were inserted separately upstream of the aureobasidin A resistance gene on the pAbAi vector and Rfx6 cDNA was inserted downstream of GAL4-activating domain (GAL4AD) on pGADT7 AD vector. The interactions between GIP promoter fragments and

Rfx6-GAL4AD protein were assayed using the aureobasidin A resistance gene reporter system. First, *S. cerevisiae* Y1HGold (*MATα, ura3-52, his3-200, ade2-101, trp1-901, leu2-3, 112, gal4Δ, gal80Δ, met-MEL1*) were transformed by GIP promoter-fragment-inserted pAbAi plasmid (pAbAi-fragment a, b, c, and d), and spread on the synthetic medium with dextrose (SD) (without uracil) and incubated for 1 week at 30°C. Obtained yeast was transformed by Rfx6 cDNA-inserted pGADT7 AD plasmid (pGADT7-Rfx6) and spread on the SD (without tryptophan) medium, and then incubated for 1 week at 30°C. Interaction between GIP promoter fragment and Rfx6-GAL4AD protein could be detected, and the transformant was grown on SD (without tryptophan) medium containing 600 ng / ml aureobasidin A.

GIP promoter activity— 1 x 10^6 STC-1 cells were co-transfected with pGL4.19 luciferase reporter plasmid expressing five different lengths of GIP promoter gene (Fig. 4C) and pGL4.73 renilla luciferase reporter plasmid. 48 h after transfection, luciferase and renilla activities were assayed according to the manufacturer's protocol (Promega Corporation, Madison, WI) using a GioMax 20 / 20n luminometer (Promega). Firefly luciferase activity was normalized to renilla luciferase expression and is presented as fold increase in relative light units over samples transfected with pGL4.19. All samples were analyzed in duplicate.

Analysis— The results are given as mean ± standard error (SEM, n = number of mice). Statistical significance was determined using paired and unpaired Student's t-test and analysis of variance (ANOVA). $P \leq 0.05$ was considered significant.

RESULTS

Visualization and isolation of K-cells using GIP-GFP mice— GIP-GFP mice were generated for the purpose of visualizing enteroendocrine K-cells (Fig. 1A). The mouse GIP gene is composed of 6 exons. The targeting vector for GIP-GFP mice was designed so that EGFP cDNA is fused with exon 3 in the GIP gene. Prepro-GIP consists of 144 amino acids (Fig. 1B) and PC1/3 and PC2 cleave prepro-GIP, generating GIP (1-42) and GIP (1-30), respectively. In GIP-GFP mice, the fusion protein retains the signal peptide, but does not have the GIP (1-42) sequence nor the PC1/3 and PC2 cleavage sites. Accordingly, GIP-GFP mice express GIP signal peptide-GFP fusion protein (280 amino acids). GFP fluorescence was observed in the small intestine of GIP-GFP heterozygous mice (Fig. 1C) and GIP-GFP homozygous mice (data not shown).

Immunohistochemical analysis was performed to assess localization of GFP-expressing cells and GIP-expressing cells using anti-GFP and anti-GIP antibodies, respectively, in the upper small intestine of wild-type and GIP-GFP heterozygous and homozygous mice (Fig. 1D). GFP-expressing cells are present in the intestine of GIP-GFP heterozygous and homozygous mice and GIP-expressing cells are present in the intestine of both wild-type and GIP-GFP heterozygous mice. However, in GIP-GFP homozygous mice, no GIP-expressing cells were found. The GFP-expressing cells were identical to the GIP-expressing cells in GIP-GFP heterozygous mice. We then examined the fasting plasma GIP levels in the three types of mice (Fig. 1E). GIP levels were significantly lower in GFP-GFP heterozygous mice compared to those in wild-type mice. GIP levels of GIP-GFP homozygous mice were not detectable. These results indicate that GIP-GFP heterozygous mice have only one normal GIP gene and that GIP-GFP homozygous mice have no normal GIP gene.

Next, GFP-positive cells were purified by a flow cytometry system. GFP-positive cells and GFP-negative cells from upper small intestinal epithelium of GIP-GFP heterozygous mice were separated and collected. GFP mRNA and GIP mRNA were highly expressed in GFP-positive cells (Fig. 1F). In microarray analysis, the expression levels of GIP mRNA were much higher in GFP-positive cells than those in GFP-negative cells (GFP-positive cells (n=3) 12951.55 $\pm$ 335.77 vs. GFP-negative cells (n=3) 1763.61 $\pm$ 142.65; $P \leq 0.001$). These results demonstrate that the GFP-positive cells in the intestinal epithelium of GIP-GFP mice are K-cells.

Transcription factor Rfx6 is expressed exclusively in K-cells— Microarray analysis data revealed that mRNA of the transcription factor Rfx6 is highly expressed in GFP-positive cells (GFP-positive cells (n=3) 2613.4 ± 341.9 vs. GFP-negative cells (n=3) 24.0 ± 6.7; $P \leq 0.05$). As seven members of the Rfx family were identified previously, we evaluated the expression of these mRNAs in mouse islets, GFP-positive cells (K-cells), and mouse small intestinal cell line STC-1 (Fig. 2A). All of the Rfx genes, except for Rfx4, were expressed in islets as shown in a previous study (20). Rfx3, Rfx6, and Rfx7 were expressed in GFP-positive cells, but no Rfx mRNAs were detected in the GFP-negative cells. In semi-quantitative RT-PCR data, the expression levels of Rfx6 were extremely higher in GFP-positive cells than those in GFP-negative cells, while the expression levels of Rfx3 and Rfx7 were similar (Fig. 2B). Immunohistochemistry confirmed that Rfx6-expressing cells correspond to GFP-expressing cells (Fig. 2C), demonstrating that Rfx6 is expressed exclusively in K-cells.

Inhibition of Rfx6 and Pdx1 expression decreases GIP expression in STC-1 cells— We then assessed the influence of Rfx6 on GIP expression and secretion by using STC-1 cells. Rfx6 mRNA expression was confirmed in STC-1 cells by RT-PCR (Fig. 2A). The Rfx6-expressing cells were similarly located in the GIP-expressing cells by immunohistochemistry (Fig. 2D). By treatment with Rfx6 siRNA, Rfx6 mRNA expression was inhibited by 70% (Fig. 2E). In the same condition, mRNA expression, cellular content, and secretion of GIP were significantly decreased while those of GLP-1 were similar to control (Fig. 2E, 2F and 2G), indicating that Rfx6 increases GIP mRNA expression, cellular content, and secretion. On the other hand, Pdx1 is reported to be an important transcriptional factor for producing GIP in K-cells (17, 18), although its expression levels were similar in GFP-positive and GFP-negative cells (Fig. 3A). To examine the effect of Pdx1 on incretin expression and secretion, mRNA expression, cellular content, and secretion of GIP and GLP-1 were measured in Pdx1-knockdown STC-1 cells by using siRNA. Pdx1 mRNA expression was confirmed in STC-1 cells by RT-PCR (Fig. 3B). The expression levels of Pdx1 mRNA were decreased by 50% in STC-1 cells treated with Pdx1 siRNA (Fig. 3C). GIP mRNA expression, cellular content, and secretion were significantly decreased, while GLP-1 mRNA expression, cellular content, and secretion were somewhat increased in STC-1 cells treated with Pdx1 siRNA (Fig. 3C, 3D, and 3E). The expression levels of Rfx6 mRNA were significantly decreased in the cells (Fig. 3C).

Interaction of Rfx6 and GIP gene— We assessed the interaction of the Rfx6 and GIP gene by one-hybrid assay. Four fragments of GIP promoter were constructed (Fig. 4A). Rfx6 effectively bound to fragment b (5216-6512 base pairs (bp) upstream of GIP promoter) (Fig. 4B). In the luciferase promoter assay, GIP promoter activity of fragments A and B containing 5216-6512 bp upstream of GIP promoter was high, while the activities of GIP promoter C, D and E were significantly decreased (Fig. 4D). These results suggest that Rfx6 binds to the region 5216-6512 bp upstream of the GIP promoter, which regulates the GIP promoter activity. Furthermore, Rfx6 was over-expressed in STC-1 cells by transfection of Rfx6 expression plasmids. The expression levels of Rfx6 mRNA levels were significantly higher in Rfx6 over-expressing cells compared to control (Fig. 4E). Rfx6 had no effect on the expression levels of to Pdx1 mRNA. GIP mRNA expression levels were significantly increased in Rfx6 over-expressing cells, but GLP-1 mRNA expression levels were not (Fig. 4F).

HFD-feeding increases GIP secretion and induces obesity and insulin hypersecretion in GIP-GFP heterozygous mice— To investigate the mechanisms of GIP hypersecretion in HFD-induced obesity *in vivo*, GIP-GFP heterozygous mice were fed CFD or HFD for 8 weeks. One week after starting with these diets, the body weight of the HFD group was significantly increased compared to that of CFD group (Fig. 5A). There was no difference in food and water intake between the CFD and HFD group (data not shown). After CHD- or HFD-feeding for 8 weeks, OGTTs were performed.

Blood glucose levels were significantly increased at 60 and 120 min during OGTT in HFD group (Fig. 5B). Insulin levels also were significantly increased in HFD group (Fig. 5C). Insulin secretion (AUC-insulin) of HFD group was increased about 5.5-fold compared to that of CFD group (CFD group (n=6) 38221 $\pm$ 238 vs. HFD group (n=6) 211835 $\pm$ 456; $P \leq 0.001$). GIP concentrations of HFD group at 15, 30, and 60 min were increased significantly compared to those of CFD group (Fig. 5D). GIP secretion (AUC-GIP) of HFD group was increased about 1.5-fold compared to that of CFD group (CFD group (n=6) 7368 $\pm$ 123 vs. HFD group (n=6) 10531 $\pm$ 216; $P \leq 0.05$) These results show that HFD-feeding increases GIP secretion and induces obesity and insulin hypersecretion in GIP-GFP heterozygous mice, which have only one normal GIP gene.

GIP hypersecretion in HFD-induced obese mice is not due to increase of K-cell number but to increase of GIP expression in K-cells— To determine whether GIP hypersecretion involves an increased number of K-cells in HFD-fed GIP-GFP heterozygous mice, the number and localization of the K-cells in the upper small intestine were estimated and compared. The length of mucous membrane and the number and localization of K-cells examined by immunohistochemistry were similar in the CFD and HFD group (Fig. 5E, 5F, and 5G). Flow cytometry analysis also showed no difference in K-cell number between the two groups (Fig. 5H). On the other hand, GIP content in upper small intestine was significantly increased in HFD group compared to that in CFD group (Fig. 5I). In addition, in K-cells purified using flow cytometry, the expression levels of GIP mRNA were almost 10-fold higher in HFD group than those in CFD group (Fig. 5J). These results demonstrate that GIP hypersecretion under HFD-induced obesity is not due to an increase in K-cell number but to an increase of GIP mRNA expression and content in K-cells.

Rfx6 and Pdx1 mRNA levels were increased in K-cells of HFD-induced obese mice— We also assessed the expression of other candidate genes in K-cells (GFP-positive cells) (Fig. 5K) and non-K-cells (GFP-negative cells). Both Rfx6 and Pdx1 mRNA levels were increased in K-cells of HFD group compared to those in K-cells of CFD group, but the mRNA expression levels of Rfx3 and Rfx7 were not. Other Rfx transcriptional factors (Rfx1, 2, 4 and 5) were not detected in the K-cells of HFD-fed mice. Furthermore, none of the Rfx transcriptional factors were detected in non-K-cells. Pdx1 mRNA expression was detected in non-K-cells but there was no significant difference in the expression level between CHD group and HFD group (ratio of Pdx1 mRNA to GAPDH mRNA: CFD group (n=8) 0.47 $\pm$ 0.15 vs. HFD group (n=8) 0.26 $\pm$ 0.08; $P = 0.24$). These results strongly suggests that an increase in Rfx6 expression as well as Pdx1 expression in K-cells stimulate GIP mRNA expression and content in K-cells of HFD-fed obese mice.

DISCUSSION

Analysis of K-cells *in vivo* has been impossible due to inability to isolate the GIP-producing K-cells from intestinal epithelium. In the present study, GIP-GFP mice enabled sorting GFP-positive cells as K-cells and revealed that the transcription factor Rfx6 is expressed exclusively in K-cells by microarray analysis and RT-PCR (Fig. 2B). Rfx3 and Rfx7 also were detected in K-cells by RT-PCR, but there were no significant differences in their expression between K-cells and non-K-cells (Fig. 2B). The Rfx gene family of transcription factors was first detected in mammals as regulatory factors that bind to the promoter regions of major histocompatibility complex (MHC) class II genes (21); seven types of Rfx (Rfx1-7) have so far been identified. All Rfx transcriptional factors have a winged helix DNA binding domain. Rfx1, 2, 3, 4 and 6 have a dimerization domain (22, 23), and Rfx6 forms homodimers or heterodimers with Rfx2 or Rfx3 (24, 25). Rfx6 was initially isolated from human genome sequences in 2008 (22). Serial Analysis of Gene Expression (SAGE) frequency data showed high expression of Rfx6 mRNA in pancreas, liver, and heart, and RT-PCR analysis showed high expression of Rfx6 mRNA in human pancreas and intestine (20). On the other hand, it is known that Rfx3 mRNA is expressed in brain, placenta,

pancreas, and pituitary, and that Rfx3 directly regulates the promoters of GLUT2 and glucokinase in pancreatic β-cells (26). Rfx7 is known to be expressed in many different tissues. Rfx3- and Rfx6-deficient mice were generated previously and none of the endocrine cells, excluding pancreatic polypeptide (PP)-expressing cells, are detected in the islets of these mice (20, 27). These results suggest that Rfx3 and Rfx6 play a critical role in generating the endocrine cells in islets, but it is unknown whether they are associated with generation of enteroendocrine cells such as K-cells and L-cells. We examined incretin mRNA expression and content under inhibition of Rfx6 expression in STC-1 cells. Other incretin GLP-1 mRNA expression and content were preserved in Rfx6-knockdown STC-1 cells. On the other hand, GIP mRNA expression and content were significantly decreased in the cells (Fig. 2E, 2F, and 2G). In addition, Rfx3 expression tended to be higher in GFP-positive cells than that in GFP-negative cells (Fig. 2B), but GIP mRNA expression, content, and secretion were not changed in Rfx3-knockdown STC-1 cells (data not shown). These results suggest that Rfx6 expressed exclusively in K-cells plays an important role in GIP expression, cellular content, and secretion in K-cells. In addition, we examined the effect of Rfx6 on the GIP gene and found that Rfx6 binds to the region 5216-6512 bp upstream of GIP promoter gene (Fig. 4D) and that Rfx6 increased GIP mRNA expression in STC-1 cells (Fig. 4F). Further study is needed to clarify the regulatory mechanism of GIP promoter activity by Rfx6. In previous studies, characterization of K-cells and microarray analysis were done using purified K-cells from the intestine of transgenic mice expressing a yellow fluorescent protein (YFP) under control of the 200 kb rat GIP promoter (28, 29), but Rfx6 expression in K-cells was not reported. The reason such a long promoter is required for specific expression of YFP in K-cells is not known, but it suggests that regulation of GIP gene expression is under complex control. In the present study, we established GIP-GFP mice in which GFP is under an endogenous, native promoter. Using these GIP-GFP mice, we were able to determine that Rfx6 is expressed exclusively in K-cells.

In the previous studies, Pdx1 expression was detected in K-cells and Pdx1-deficient mice showed a greatly decreased number of GIP-expressing cells in the intestine (18, 19). It also has been reported that Pdx1 binds at 150 bp upstream of GIP promoter and activates GIP promoter in STC-1 cells and that Pdx1 expression is essential for producing GIP in K-cells (18, 19). We found that there was no significant difference in Pdx1 mRNA expression between upper small intestinal K-cells and non-K-cells (Fig. 3A). These findings suggest the possibility that Rfx6 specifically expressed in K-cells plays a critical role in differentiation and GIP production of K-cells in collaboration with Pdx1**.** It was reported that Rfx6 mRNA expression is regulated by transcription factor Neurogenin 3 (Ngn3) in fetus pancreas (30). In another report, no colocalization of Pdx1-expressing cells and Rfx6-expressing cells was found in mouse fetus pancreas using immunohistchemistry analysis**,** and Pdx-1 expression was decreased in pancreas of Rfx6-defficient mice (20). In the present study, Pdx1 mRNA expression levels were not changed not in only Rfx6-knockdown STC-1 cells but also in Rfx6 over-expressing STC-1 cells, while Rfx6 expression levels were significantly decreased in Pdx1-knockdown STC-1 cells (Fig. 2E, Fig. 3C, and Fig. 4E). These results suggest that Rfx6 expression is at least in part regulated by Pdx1.

Increased blood GIP levels in obesity have been reported in several studies (7, 14, 15, 16). There is a report that healthy human subjects administered high-fat food for 2 weeks showed increased plasma GIP levels without developing obesity, suggesting that GIP hypersecretion precedes obesity (31). GIP is released from K-cells into circulation in response to various nutrients (32, 33, 34). Measurement of total GIP and total GLP-1 levels in humans challenged with glucose or meal shows that the postprandial plasma GIP level is greatly augmented when a meal containing abundant fat rather than simple glucose is consumed (35, 36). This suggests that intake of HFD increases GIP secretion and strengthens both direct and indirect effects of GIP on energy accumulation in adipose tissue. We previously reported that

both GIP levels after glucose loading and BMI have a positive correlation in healthy subjects (37). In the present study, GIP levels during OGTT were increased in obese GIP-GFP heterozygous mice compared to those in lean GIP-GFP heterozygous mice, even though GIP-GFP heterozygous mice have only one normal GIP gene, indicating these mice represent a useful model for analysis of the mechanisms involved in the augmented GIP secretion in HFD-induced obesity. A previous study reported that augmentation of GIP secretion in HFD-feeding conditions is due to increased K-cell number (38). In that report, agglomerates of Pdx1- and GIP-double expressing cells were found inside the duodenal mucosa of obese rats after HFD-feeding. In the present study, however, we could not detect agglomerates of K-cells or an increase of K-cell number in duodenum or upper small intestine of HFD-fed GIP-GFP heterozygous mice by immunohistochemistry and flow cytometry analysis. The reason for this discrepancy could be difference of species, food composition, and / or duration of the HFD-feeding period. In our study, GIP content was significantly increased in the upper small intestine of HFD-fed mice compared to that in CFD-fed mice, and GIP mRNA expression was increased in K-cells of HFD-fed mice. These results suggest that GIP hypersecretion in HFD-induced obese mice is due to increased GIP expression in K-cells. In this condition, the expression levels of Rfx6 and Pdx1 mRNA were significantly increased in K-cells (Fig. 5K). As Rfx6 and Pdx1 were found to be important transcriptional factors in producing GIP in K-cells in our results using Rfx6 knockdown and over-expression and in previous *in vitro* studies for Pdx1, an increase in Rfx6 and Pdx1 expressions might well be involved in GIP hypersecretion in K-cells in HFD-induced obese mice.

In conclusion, gene analysis of K-cells isolated from GIP-GFP mice enables identification of the transcription factor Rfx6 which is expressed exclusively in K-cells and is involved in the regulation of GIP expression. We also show that expression of Rfx6 and Pdx1 is upregulated in K-cells of HFD-induced obese mice, which suggests that induction of Rfx6 as well as Pdx1 plays a critical role in GIP hypersecretion in HFD-induced obesity.

REFERENCES

1. Reaven GM. (1988) Banting lecture 1988. Role of insulin resistance in human disease. *Diabetes.* **37**, 1066-1084
2. Kahn BB, Flier JS. (2000) Obesity and insulin resistance. *J Clin Invest.* **106**, 473-481
3. Lemieux I, Pascot A, Couillard C, Lamarche B, Tchernof A, Almeras N, Bergeron J, Gaudet D, Tremblay G, Prud'homme D, Nadeau A, Despres JP. (2000) Hypertriglyceridemic waist: A marker of the atherogenic metabolic triad (hyperinsulinemia; hyperapolipoprotein B; small, dense LDL) in men? *Circulation.* **102**, 179-184
4. Pederson RA. (1994) Gastric inhibitory polypeptides. *Gut Peptides: Biochemistry and Physiology*, edited by Walsh JH and Dockray GJ; Raven Press, NY
5. Drucker DJ. (1998) Glucagon-like peptides. *Diabetes.* **47**, 159-169
6. Seino Y, Fukushima M, Yabe D. (2010) GIP and GLP-1, the two incretin hormone: Similalities and differernce. *J Diabet Invest*. **1**, 8-23
7. Miyawaki K, Yamada Y, Ban N, Ihara Y, Tsukiyama K, Zhou H, Fujimoto S, Oku A, Tsuda K, Toyokuni S, Hiai H, Mizunoya W, Fushiki T, Holst JJ, Makino M, Tashita A, Kobara Y, Tsubamoto Y, Jinnouchi T, Jomori T, Seino Y. (2002) Inhibition of gastric inhibitory polypeptide signaling prevents obesity. *Nat Med.* **8**, 738-742
8. Tsukiyama K, Yamada Y, Yamada C, Harada N, Kawasaki Y, Ogura M, Bessho K, Li M, Amizuka N, Sato M, Udagawa N, Takahashi N, Tanaka K, Oiso Y, Seino Y. (2006) Gastric inhibitory polypeptide as an endogenous factor promoting new bone formation following food ingestion. *Mol Endocrinol.* **20**, 1644-1651
9. Miyawaki K, Yamada Y, Yano H, Niwa H, Ban N, Ihara Y, Kubota A, Fujimoto S, Kajikawa M, Kuroe A, Tsuda K, Hashimoto H, Yamashita T, Jomori T, Tashiro F, Miyazaki J, Seino Y. (1999) Glucose intolerance caused by a defect in the entero-insular axis: a study in gastric inhibitory polypeptide receptor knockout mice. *Proc Natl Acad Sci USA*. **96**, 14843-14847

10. Harada N, Yamada Y, Tsukiyama K, Yamada C, Nakamura Y, Mukai E, Hamasaki A, Liu X, Toyoda K, Seino Y, Inagaki N. (2008) A novel GIP receptor splice variant influences GIP sensitivity of pancreatic beta-cells in obese mice. *Am J Physiol Endocrinol Metab.* **294**, 61-68
11. Usdin TB, Mezey E, Button DC, Brownstein MJ, Bonner TI. (1993) Gastric inhibitory polypeptide receptor, a member of the secretin-vasoactive intestinal peptide receptor family, is widely distributed in peripheral organs and the brain. *Endocrinology.* **133**, 2861-2870
12. Hauner H, Glatting G, Kaminska D, Pfeiffer EF. (1988) Effects of gastric inhibitory polypeptide on glucose and lipid metabolism of isolated rat adipocytes. *Ann Nutr Metab.* **32**,282-288
13. Song DH, Getty-Kaushik L, Tseng E, Simon J, Corkey BE, Wolfe MM. (2007) Glucose-dependent insulinotropic polypeptide enhances adipocyte development and glucose uptake in part through Akt activation. *Gastroenterology.* **133**, 1796-805
14. Bailey CJ, Flatt PR, Kwasowski P, Powell CJ, Marks V. (1986) Immunoreactive gastric inhibitory polypeptide and K cell hyperplasia in obese hyperglycaemic (ob/ob) mice fed high fat and high carbohydrate cafeteria diets. *Acta Endocrinol.* **112**, 224-229
15. Flatt PR, Bailey CJ, Kwasowski P, Swanston-Flatt SK, Marks V. (1983) Abnormalities of GIP in spontaneous syndromes of obesity and diabetes in mice. *Diabetes.* **32**, 433-435
16. Creuzfeldt W, Ebert R, Willms B, Frerichs H, Brown JC. (1983) Gastric inhibitory polypeptide (GIP) and insulin in obesity: increased response to stimulation and defective feedback control of serum levels. *Diabetologia.* **14**, 15-24
17. Jonsson, J., Carlsson, L., Edlund, T., Edlund, H. (1994) Insulin-promoter-factor 1 is required for pancreas development in mice. *Nature.* **371**, 606-609
18. Jepeal LI, Fujitani Y, Boylan MO, Wilson CN, Wright CV, Wolfe MM. (2005) Cell-specific expression of glucose-dependent-insulinotropic polypeptide is regulated by the transcription factor PDX-1. *Endocrinology.* **146**, 383–391
19. Fujita Y, Chui JW, King DS, Zhang T, Seufert J, Pownall S, Cheung AT, Kieffer TJ. (2008) Pax6 and Pdx1 are required for production of glucose-dependent insulinotropic polypeptide in proglucagon-expressing L cells. *Am J Physiol Endocrinol Metab.* **295**, 648-657
20. Smith SB, Qu HQ, Taleb N, Kishimoto NY, Scheel DW, Lu Y, Patch AM, Grabs R, Wang J, Lynn FC, Miyatsuka T, Mitchell J, Seerke R, Désir J, Eijnden SV, Abramowicz M, Kacet N, Weill J, Renard ME, Gentile M, Hansen I, Dewar K, Hattersley AT, Wang R, Wilson ME, Johnson JD, Polychronakos C, German MS. (2010) Rfx6 direct islet formation and insulin production in mice and humans. *Nature.* **463**, 775-780
21. Reith W, Barras E, Satola S, Kobr M, Reinhart D, Sanchez CH, Mach B. (1989) Cloning of the major histiocompatibility complex class II promoter binding protein affected heredity defect in class II gene regulation. *Proc Natl Acad Sci USA.* **86**, 4200-4204
22. Aftab S, Semenec L, Chu JS, Chen N. (2008) Identification and characterization of novel human tissue-specific RFX transcription factors. *BMC Evol Biol.* **8**, 226-236
23. Katan-Khaykovich Y, Shaul Y. (1998) RFX1, a single DNA-binding protein with a split dimerization domain, generates alternative complexes. *J Biol Chem.* **273**, 24504-24512
24. Rual JF, Venkatesan K, Hao T, Hirozane-Kishikawa T, Dricot A, Li N, Berriz GF, Gibbons FD, Dreze M, Ayivi-Guedehoussou N, Klitgord N, Simon C, Boxem M, Milstein S, Rosenberg J, Goldberg DS, Zhang LV, Wong SL, Franklin G, Li S, Albala JS, Lim J, Fraughton C, Llamosas E, Cevik S, Bex C, Lamesch P, Sikorski RS, Vandenhaute J, Zoghbi HY, Smolyar A, Bosak S, Sequerra R, Doucette-Stamm L, Cusick ME, Hill DE, Roth FP, Vidal M. (2005) Towards a proteome-scale map of the human protein–protein interaction network. *Nature.* **437**, 1173-1178
25. Rhodes DR, Tomlins SA, Varambally S, Mahavisno V, Barrette T, Kalyana-Sundaram S, Ghosh D, Pandey A, Chinnaiyan AM. (2005) Probabilistic model of the human protein-protein interaction network. *Nat Biotechnol.* **23**, 951-959
26. Ait-Lounis A, Bonal C, Seguín-Estévez Q, Schmid CD, Bucher P, Herrera PL, Durand B, Meda P, Reith W. (2010) The transcription factor Rfx3 regulates beta-cell differentiation, function, and glucokinase expression. *Diabetes.* **59**, 1674-1685

27. Ait-Lounis A, Baas D, Barras E, Benadiba C, Charollais A, Nlend Nlend R, Liègeois D, Meda P, Durand B, Reith W. (2007) Novel function of ciliogenic transcription factor RFX3 in development of the endocrine pancreas. *Diabetes.* **56**, 950-959
28. Parker HE, Habib AM, Rogers GJ, Gribble FM, Reimann F. (2009) Nutrient-dependent secretion of glucose-dependent insulinotropic polypeptide from primary murine K cells. *Diabetologia.* **52**, 289-298
29. Habib AM, Richards P, Cairns LS, Rogers GJ, Bannon CA, Parker HE, Morley TC, Yeo GS, Reimann F, Gribble FM. (2012) Overlap of endocrine hormone expression in the mouse intestine revealed by transcriptional profiling and flow cytometry. *Endocrinology*. **153**, 3054-3065
30. Soyer J, Flasse L, Raffelsberger W, Beucher A, Orvain C, Peers B, Ravassard P, Vermot J, Voz ML, Mellitzer G, Gradwohl G. (2010) Rfx6 is an Ngn3-dependent winged helix transcription factor required for pancreatic islet cell development. *Development.* **137**, 203-212
31. Brøns C, Jensen CB, Storgaard H, Hiscock NJ, White A, Appel JS, Jacobsen S, Nilsson E, Larsen CM, Astrup A, Quistorff B, Vaag A. (2009) Impact of short-term high-fat feeding on glucose and insulin metabolism in young healthy men. *J Physiol.* **587**, 2387-2397
32. Yoder SM, Yang Q, Kindel TL, Tso P. (2010) Differential responses of the incretin hormones GIP and GLP-1 to increasing doses of dietary carbohydrate but not dietary protein in lean rats. *Am J Physiol Gastrointest Liver Physiol*. **299**, 476-485
33. Brown JC, Dryburgh JR, Ross SA, Dupré J. (1975) Identification and actions of gastric inhibitory polypeptide. *Recent Prog Horm Res*. **31**, 487-532
34. Falko JM, Crockett SE, Cataland S, Mazzaferri EL. (1975) Gastric inhibitory polypeptide (GIP) stimulated by fat ingestion in man. *J Clin Endocrinol Metab.* **41**, 260-265
35. Vollmer K, Holst JJ, Baller B, Ellrichmann M, Nauck MA, Schmidt WE, Meier JJ. (2008) Predictors of incretin concentrations in subjects with normal, impaired, and diabetic glucose tolerance. *Diabetes*. **57**, 678-687
36. Yamane S, Harada N, Hamasaki A, Muraoka A, Joo E, Suzuki K, Nasteska D, Tanaka D, Ogura M, Harashima S, Inagaki N. (2012) Effects of glucose and meal ingestion on incretin secretion in Japanese subjects with normal glucose tolerance. *J Diabtes Invest.* **3**, 81-5
37. Harada N, Hamasaki A, Yamane S, Muraoka A, Joo E, Fujita K, Inagaki N. (2011) Plasma GIP and GLP-1 levels are associated with distinct factors after glucose loading in Japanese subjects. *J Diabtes Invest.* **2**,193-199
38. Gniuli D, Calcagno A, Dalla Libera L, Calvani R, Leccesi L, Caristo ME, Vettor R, Castagneto M, Ghirlanda G, Mingrone G. (2010) High-fat feeding stimulates endocrine, glucose-dependent insulinotropic polypeptide (GIP)-expressing cell hyperplasia in the duodenum of Wistar rats. *Diabetologia.* **53**, 2233–2240

Acknowledgments — The authors thank Prof. Douglas Hanahan, University of California, San Francisco, for kindly providing the STC-1 cells. The authors also thank Dr. Yoshitaka Hayashi, Research Institute of Environmental Medicine, Nagoya University, for helpful suggestions regarding the study. Mouse Anti-GIP antibody was kindly provided by Millipore Merck.

FOOTNOTES

*This study was supported by Scientific Research Grants from the Ministry of Education, Culture, Sports, Science, and Technology, Japan, and from the Ministry of Health, Labor, and Welfare, Japan. This study was also supported by Scientific Research Grants from Japan Diabetes Foundation.

Corresponding Author. Address: Nobuya Inagaki, Department of Diabetes and Clinical Nutrition, Graduate School of Medicine, Kyoto University, 54 Kawahara-cho, Shogoin, Sakyo-ku, Kyoto 606-8507, Japan. Tel: +81(Japan)-75-751-3562, Fax: +81(Japan)-75-751-6601
E-mail: inagaki@metab.kuhp.kyoto-u.ac.jp

FIGURE LEGENDS

FIGURE 1. Gene construct of GIP-GFP mic**e.** A. Wild-type GIP allele and targeted allele of GIP-GFP. EGFP-polyA-loxp-Neo-loxp cassette was inserted into exon 3 of wild-type GIP gene. B. Prepro GIP protein and GIP-GFP fusion protein. SP: signal peptide. Open triangle: PC1/3 cleavage site, Closed triangle: PC2 cleavage site, Dotted line: amino acids of signal peptide, Solid line: translated protein from exon 3. C. Microscopic images of upper small intestine in GIP-GFP heterozygous mice (bright field image and fluorescence image). D. Immunohistchemical images of upper small intestine in wild-type (WT), GIP-GFP heterozygous ($GIP^{gfp/+}$), and homozygous mice ($GIP^{gfp/gfp}$). Green: GFP-expressing cells, Red: GIP-expressing cells, Yellow: Merged image. E. Fasting plasma GIP levels in WT, $GIP^{gfp/+}$, and $GIP^{gfp/gfp}$ mice. F. GFP mRNA and GIP mRNA levels in GFP-positive cells (n=5-6) and GFP-negative cells (n=5-6). $*P \leq 0.05$, $**P \leq 0.01$, $***P \leq 0.001$

FIGURE 2. The effect of Rfx6 on mRNA expression, cellular content, and secretion of GIP in STC-1 cells. A. mRNA expression for Rfx genes 1-7 in islets, GFP-negative cells, GFP-positive cells, and STC-1 cells by PCR. B. Rfx3, Rfx6, and Rfx7 mRNA levels in GFP-positive cells (n=8-10) and GFP-negative cells (n=8-10). C. Immunohistchemical images of upper small intestine in GIP-GFP heterozygous mice. Green: GFP-expressing cells, Red: Rfx6-expressing cells, Yellow: Merged image. D. Immunohistchemical images of STC-1 cells. Green: GIP-expressing cells, Red: Rfx6-expressing cells, Yellow: Merged image. E. Rfx6, GIP, GLP-1 and Pdx1 mRNA levels in Rfx6 knockdown STC-1 cells (n=4). F and G. Incretin content and secretion in Rfx6 knockdown STC-1 cells (n=4). $*P \leq 0.05$, $**P \leq 0.01$, n.s., not significance.

FIGURE 3. The effect of Pdx1 on mRNA expression, cellular content, and secretion of GIP. A. Pdx1 mRNA levels in GFP-positive cells and GFP-negative cells (n=8-10). B. GIP, GLP-1, and Pdx1 mRNA expressions in STC-1 cells by RT-PCR. C. Pdx1, GIP, GLP-1, and Rfx6 mRNA levels in Pdx1 knockdown STC-1 cells (n=4). D and E. Incetin content and secretion in Pdx1 knockdown STC-1 cells (n=4). $*P \leq 0.05$, $**P \leq 0.01$, $***P \leq 0.001$, n.s., not significance.

FIGURE 4. Interaction of Rfx6 and GIP gene. A. The design of the GIP promoter fragments for one-hybrid assay. Numbers indicate nucleotides upstream from the transcription start site of GIP gene. B. Results of yeast one-hybrid assay. Only yeast transformed with both pAbAi vector containing fragment b (pAbAi–fragment b) and Rfx6 cDNA-inserted pGADT7 (pGADT7-Rfx6) was grown on SD medium. C. The design of the different length of GIP promoter gene for luciferase reporter plasmid transfected in STC-1 cells. D. Luciferase promoter assay on GIP promoter. Data are represented by ratio of relative light unit (RLU) of Fragment E (n=3-4). $*P \leq 0.05$, n.s., not significance. E and F. Pdx1, Rfx6, GIP, and GLP-1 mRNA levels in Rfx6 over-expressing STC-1 cells. $**P \leq 0.01$, $***P \leq 0.001$ vs. control, n.s., not significance.

FIGURE 5. Analysis of K-cells in the small intestine of CFD- and HFD-fed GIP-GFP heterozygous mice (Histology, flow cytometry analysis, and gene expression). A. Body weight change of CFD-fed (dashed line) and HFD-fed (continuous line) GIP-GFP heterozygous mice (n=5-7). B, C and D. Blood glucose (B), insulin (C), and GIP levels (D) during OGTT after 8 weeks of CFD- or HFD-feeding (n=5). Dashed line and white box shows CFD group, while continuous line and black box shows CFD group. $*P \leq 0.05$, $**P \leq 0.01$, $***P \leq 0.001$ vs. CFD-fed mice. E. The length of mucous membrane in upper small intestine. (n=5). F. The number of GFP-positive cells by immunohistochemistry (n=5). G. The localization of K-cells in the upper small intestine by immunohistochemistry (n=5). H. The number of K-cells in the upper small intestine by flow cytometry analysis (n=5). I. GIP content in upper small intestine (n=5-7). J. GIP mRNA levels in GFP-positive cells (n=8-10). K. Pdx1, Rfx3, Rfx6, and Rfx7 mRNA levels in GFP-positive cells (n=8-10). $*P \leq 0.05$, $**P \leq 0.01$, $***P \leq 0.001$, n.s., not significance.

Figure 1

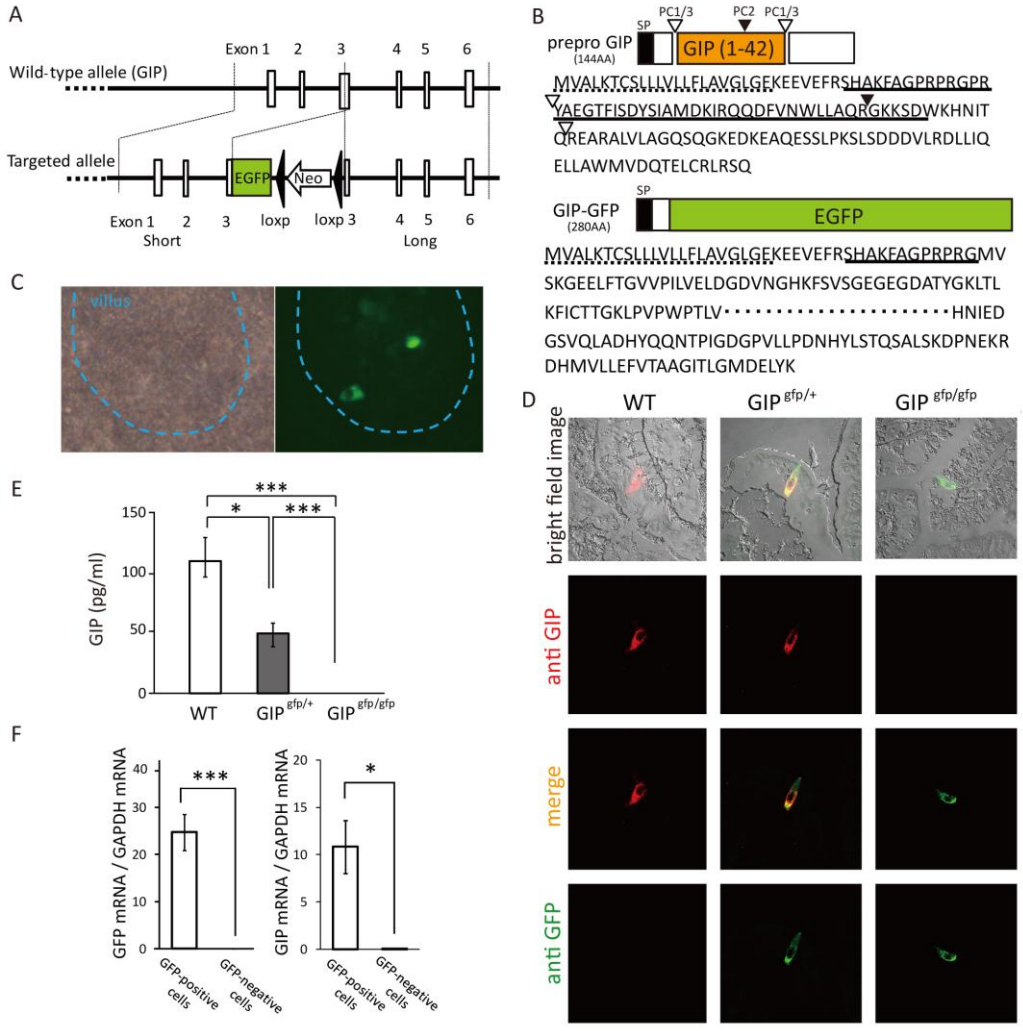
A
Exon 1 2 3 4 5 6
Wild-type allele (GIP)
Targeted allele
EGFP
Neo
Exon 1 2 3 loxp loxp 3 4 5 6
Short
Long
B
SP
PC1/3
PC2
PC1/3
prepro GIP
(144AA)
GIP (1-42)
MVALKTCSLLLVLLFLAVGLGEKEEVEFRSHAKEAGPRPRGPR
VAEGTFISDYSIAMDKIRQQDFVNWLLAQRGKKSDWKHNIT
QREARALVLAGQSQGKEDKEAQESSLPKSLSDDDVLRDLLIQ
ELLAWMVDQTELCRLRSQ
GIP-GFP
(280AA)
EGFP
MVALKTCSLLLVLLFLAVGLGEKEEVEFRSHAKEAGPRPRGMV
SKGEELFTGVVPILVELDGDVNGHKFSVSGEGEGDATYGKLTL
KFICTTGKLPVPWPTLV·····HNIED
GSVQLADHYQQNTPIGDGPVLLPDNHYLSTQSALSKDPNEKR
DHMVLLEFVTAAGITLGMDELYK
C
villus
D
WT
GIP gfp/+
GIP gfp/gfp
bright field image
anti GIP
merge
anti GFP
E
GIP (pg/ml)
150
100
50
0
***
*
***
WT
GIP gfp/+
GIP gfp/gfp
F
GFP mRNA / GAPDH mRNA
40
30
20
10
0
***
GFP-positive cells
GFP-negative cells
GIP mRNA / GAPDH mRNA
20
15
10
5
0
*
GFP-positive cells
GFP-negative cells

Figure 2

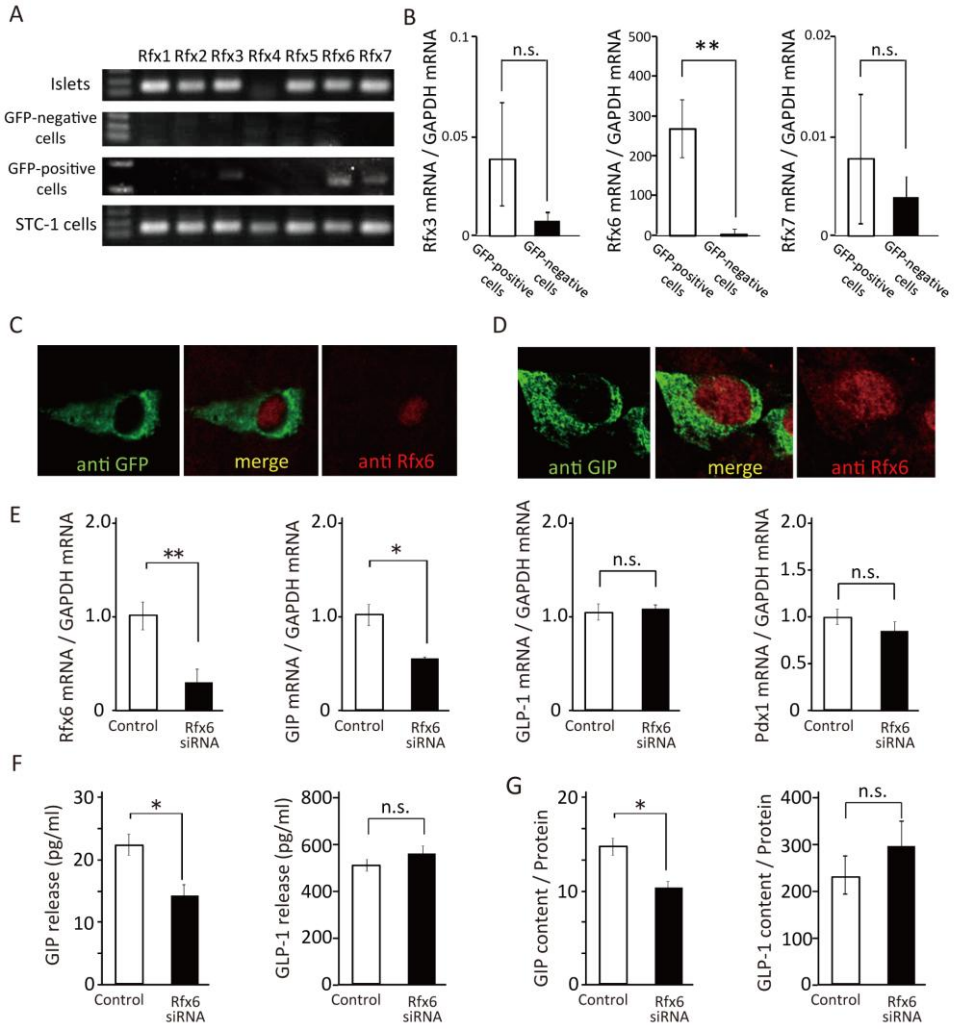
A
Rfx1 Rfx2 Rfx3 Rfx4 Rfx5 Rfx6 Rfx7
Islets
GFP-negative cells
GFP-positive cells
STC-1 cells
B
Rfx3 mRNA / GAPDH mRNA
n.s.
Rfx6 mRNA / GAPDH mRNA
**
Rfx7 mRNA / GAPDH mRNA
n.s.
GFP-positive cells
GFP-negative cells
C
anti GFP
merge
anti Rfx6
D
anti GIP
merge
anti Rfx6
E
Rfx6 mRNA / GAPDH mRNA
GIP mRNA / GAPDH mRNA
GLP-1 mRNA / GAPDH mRNA
Pdx1 mRNA / GAPDH mRNA
Control
Rfx6 siRNA
F
GIP release (pg/ml)
GLP-1 release (pg/ml)
G
GIP content / Protein
GLP-1 content / Protein

Figure 3

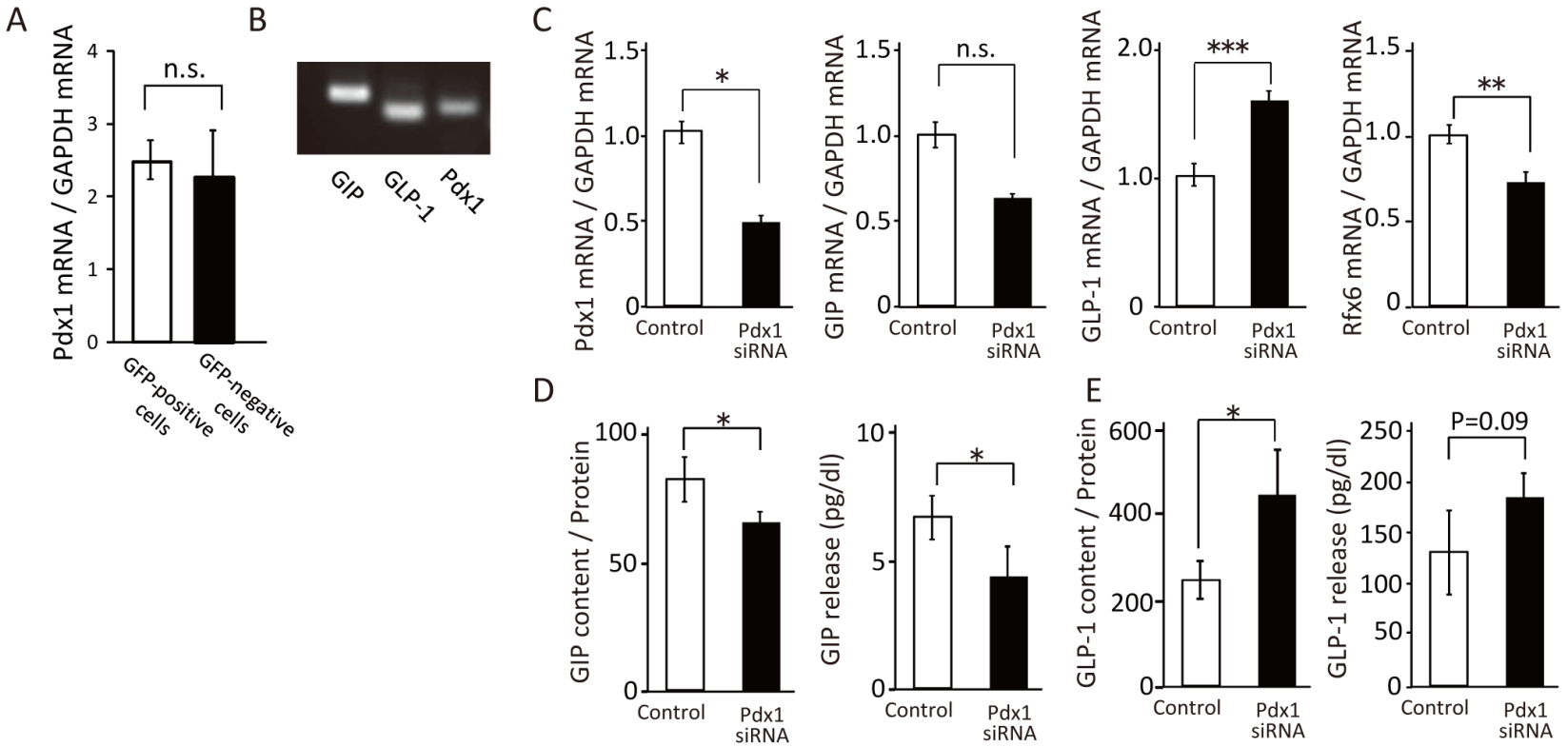
A
Pdx1 mRNA / GAPDH mRNA
n.s.
GFP-positive cells
GFP-negative cells
B
GIP
GLP-1
Pdx1
C
Pdx1 mRNA / GAPDH mRNA
*
Control
Pdx1 siRNA
GIP mRNA / GAPDH mRNA
n.s.
GLP-1 mRNA / GAPDH mRNA
***
Rfx6 mRNA / GAPDH mRNA
**
D
GIP content / Protein
GIP release (pg/dl)
E
GLP-1 content / Protein
GLP-1 release (pg/dl)
P=0.09

Figure 4

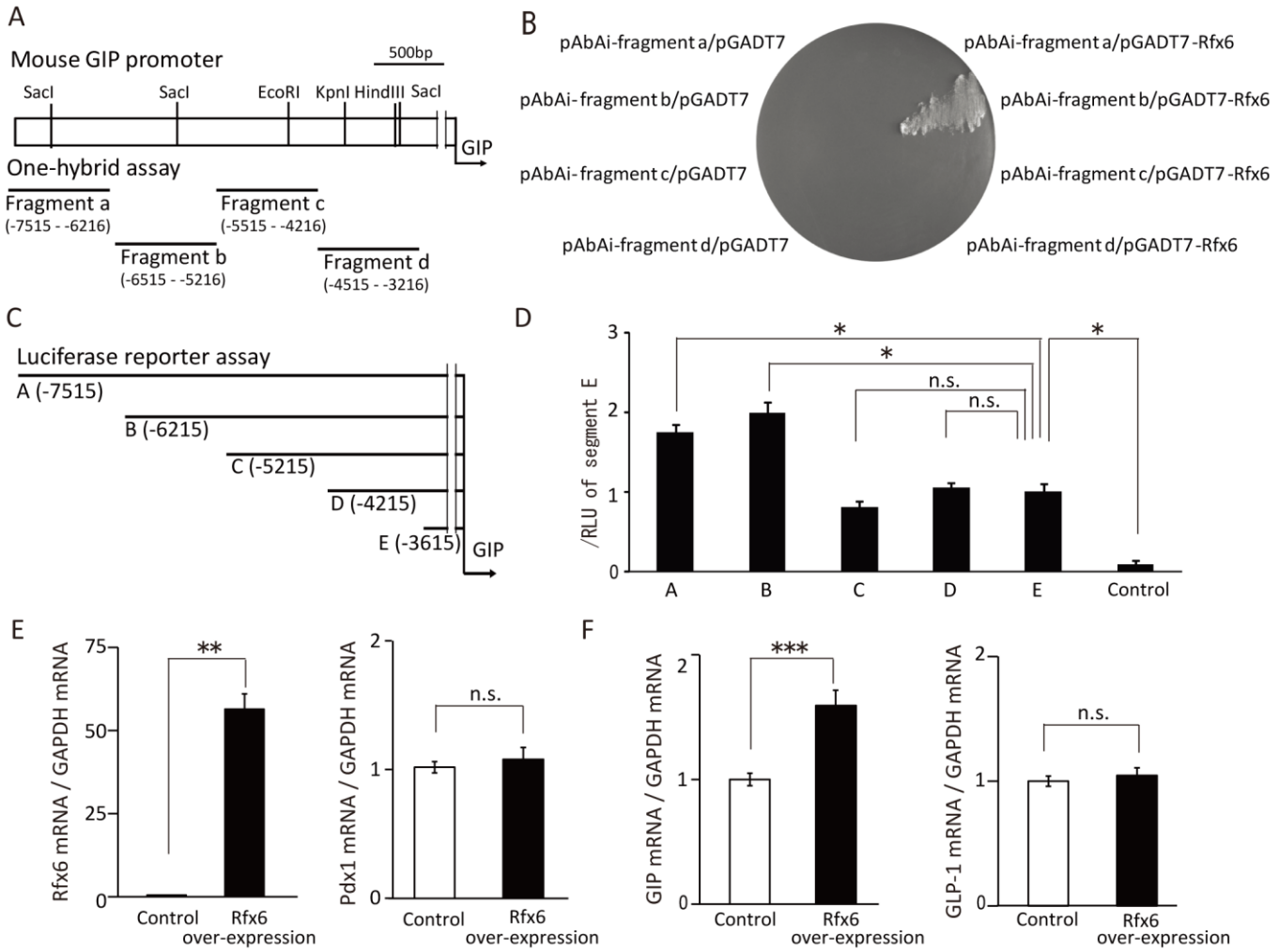
A
Mouse GIP promoter
500bp
SacI
SacI
EcoRI
KpnI
HindIII
SacI
GIP
One-hybrid assay
Fragment a
(-7515 - -6216)
Fragment b
(-6515 - -5216)
Fragment c
(-5515 - -4216)
Fragment d
(-4515 - -3216)
B
pAbAi-fragment a/pGADT7
pAbAi-fragment a/pGADT7-Rfx6
pAbAi-fragment b/pGADT7
pAbAi-fragment b/pGADT7-Rfx6
pAbAi-fragment c/pGADT7
pAbAi-fragment c/pGADT7-Rfx6
pAbAi-fragment d/pGADT7
pAbAi-fragment d/pGADT7-Rfx6
C
Luciferase reporter assay
A (-7515)
B (-6215)
C (-5215)
D (-4215)
E (-3615)
GIP
D
/RLU of segment E
*
*
*
n.s.
n.s.
A
B
C
D
E
Control
E
Rfx6 mRNA / GAPDH mRNA
**
Control
Rfx6 over-expression
Pdx1 mRNA / GAPDH mRNA
n.s.
Control
Rfx6 over-expression
F
GIP mRNA / GAPDH mRNA
***
Control
Rfx6 over-expression
GLP-1 mRNA / GAPDH mRNA
n.s.
Control
Rfx6 over-expression

Figure 5

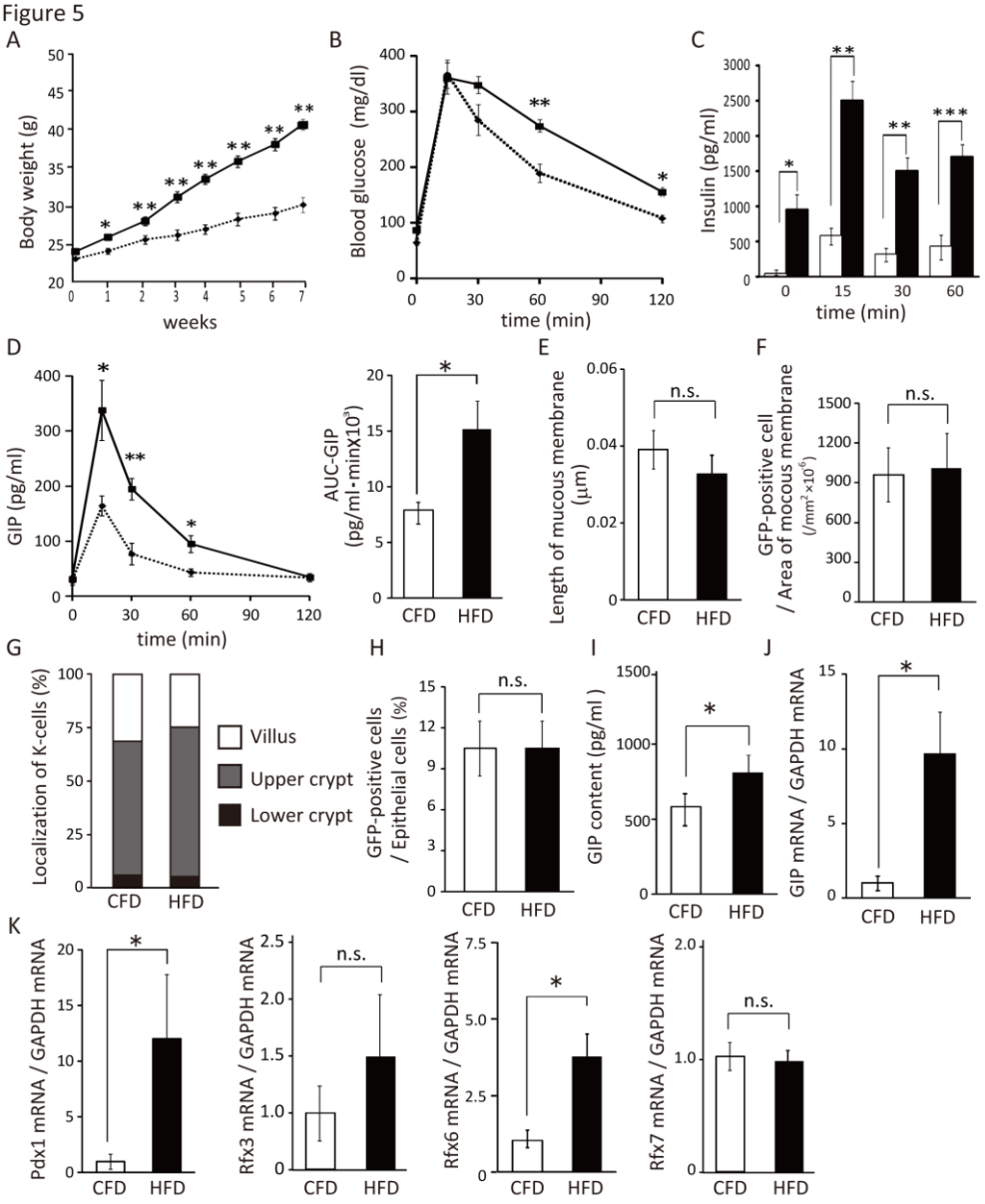
A
Body weight (g)
weeks
B
Blood glucose (mg/dl)
time (min)
C
Insulin (pg/ml)
time (min)
D
GIP (pg/ml)
time (min)
AUC-GIP (pg/ml·minX10³)
E
Length of mucous membrane (μm)
n.s.
F
GFP-positive cell / Area of mocous membrane (/mm²×10⁶)
n.s.
G
Localization of K-cells (%)
Villus
Upper crypt
Lower crypt
H
GFP-positive cells / Epithelial cells (%)
n.s.
I
GIP content (pg/ml)
J
GIP mRNA / GAPDH mRNA
K
Pdx1 mRNA / GAPDH mRNA
Rfx3 mRNA / GAPDH mRNA
n.s.
Rfx6 mRNA / GAPDH mRNA
Rfx7 mRNA / GAPDH mRNA
n.s.
CFD
HFD